

# Thiobarbiturate and barbiturate salts of pefloxacin drug: Growth, structure, thermal stability and IR-spectra

Nicolay N. Golovnev<sup>a</sup>, Maxim S. Molokeyev<sup>b,c,a\*</sup>, Maxim K. Lesnikov<sup>a</sup>, Irina V. Sterkhova<sup>d</sup>, Victor V. Atuchin<sup>e,f,g</sup>

<sup>a</sup> Siberian Federal University, 79 Svobodny Ave., Krasnoyarsk 660041, Russia

<sup>b</sup> Laboratory of Crystal Physics, Kirensky Institute of Physics, Federal Research Center KSC SB RAS, bld. 38 Akademgorodok 50, Krasnoyarsk 660036, Russia

<sup>c</sup> Department of Physics, Far Eastern State Transport University, 47 Seryshev Str., Khabarovsk 680021, Russia

<sup>d</sup> Laboratory of Physical Chemistry, Irkutsk Favorsky Institute of Chemistry, SB RAS, 1 Favorsky, Irkutsk 664033, Russia

<sup>e</sup> Laboratory of Optical Materials and Structures, Institute of Semiconductor Physics, 13 Lavrentiev Aven., Novosibirsk 630090, Russia

<sup>f</sup> Functional Electronics Laboratory, Tomsk State University, 36 Lenin Aven., Tomsk 634050, Russia

<sup>g</sup> Laboratory of Semiconductor and Dielectric Materials, Novosibirsk State University, 2 Pirogov Str., Novosibirsk 630090, Russia

\* Corresponding author:

Maxim Molokeyev

E-mail: msmolokeyev@gmail.com

Laboratory of Crystal Physics, Kirensky Institute of Physics, Federal Research Center KSC SB RAS, bld. 38 Akademgorodok 50, Krasnoyarsk 660036, Russia

Tel.: +7-391-249-45-07

---

†Electronic supplementary information (ESI) available. See DOI:xxx

## Abstract

Three new salts of pefloxacin (PefH) with thiobarbituric (H<sub>2</sub>tba) and barbituric (H<sub>2</sub>ba) acids, pefloxacinium 2-thiobarbiturate trihydrate, PefH<sub>2</sub>(Htba)·3H<sub>2</sub>O (**1**), pefloxacinium 2-thiobarbiturate, PefH<sub>2</sub>(Htba) (**2**) and bis(pefloxacinium barbiturate) hydrate, (PefH<sub>2</sub>)<sub>2</sub>(Hba)<sub>2</sub>·2.56H<sub>2</sub>O (**3**) are synthesized and structurally characterized by the X-ray single-crystal diffraction. In the structures of **1-3**, there are two intramolecular hydrogen bonds C–H...F, O–H...O and intermolecular hydrogen bonds N–H...O, O–H...O which form 2D plane network in **1** and the intermolecular hydrogen bonds N–H...O form the chains in **2** and **3**. In **1-3** the Htba<sup>−</sup> and Hba<sup>−</sup> ions are connected with PefH<sub>2</sub><sup>+</sup> only one by intermolecular hydrogen bond N–H...O. In **2** and **3**, two Htba<sup>−</sup> and Hba<sup>−</sup> ions are connected by two hydrogen bonds N–H...O. These pairs form infinite chains. All three structures are stabilized by π–π interactions between PefH<sub>2</sub><sup>+</sup> ions of the head-to-tail type. Compound **2** and **3** have been characterized by powder XRD, TG-DSC and FT-IR.

**Keywords** Thiobarbituric acid; barbituric acid; pefloxacin; salts; X-ray diffraction; infrared spectroscopy; thermal stability

## 1. Introduction

Fluoroquinolones (F<sub>x</sub>H) are the broad spectrum bactericidal antibiotics and work against both Gram-positive and Gram-negative bacteria. An important representative of this class is pefloxacin (PefH) (Fig. 1a) which widely used in clinical practice [1, 2]. It demonstrates moderate activity against anaerobes and Mycobacteria, to which the quinolone in general has low activity. The PefH is commonly used in the form of salt due to low solubility [3], for example, pefloxacinium methasulfonate, PefH<sub>2</sub>(CH<sub>3</sub>SO<sub>3</sub>). Further search for other pefloxacin salts with improved properties is of practical interest.

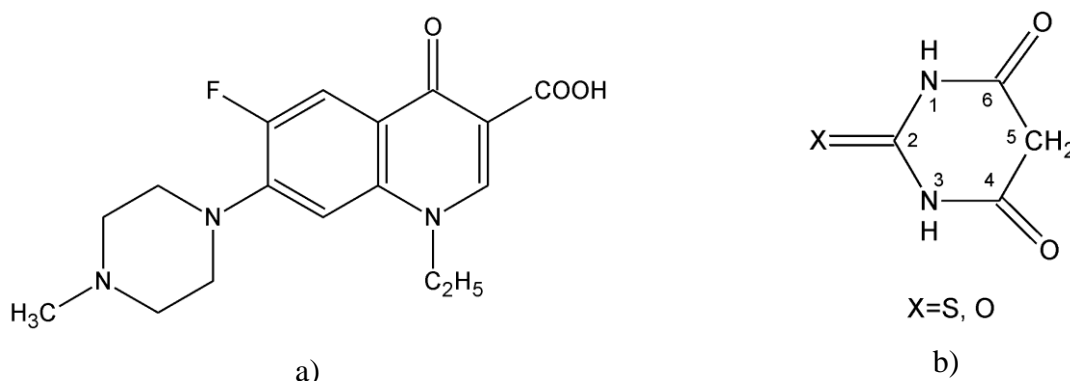


**Fig. 1** Schemes of pefloxacin (a) and barbituric acids (b): X=O in H<sub>2</sub>ba and X=S in H<sub>2</sub>tba

Barbiturates are a class of drug which used as anesthetics and sleeping agents and are utilized for the treatment different psychiatric disorders [4]. Barbituric and thiobarbituric acids (Fig. 1b) are the key compounds, which are used in synthesis of different their derivatives having important therapeutic value [5-8]. Barbituric acid (H<sub>2</sub>ba) possesses specific, relatively weak acidic properties (pK<sub>a</sub> ca. 4.03 [9]) resulting from the presence of two methylene hydrogen atoms. Thiobarbituric acid (H<sub>2</sub>tba) is a stronger acid (pK<sub>a1</sub> ca. 1.87 [10]) also resulting from the presence of two methylene hydrogen atoms. The existence of three polymorphs of anhydrous H<sub>2</sub>ba and dehydrate [11-13], and six polymorphs of anhydrous thiobarbituric acid and hydrate [14] make these molecules interesting from the viewpoint of crystal engineering. They can be used as a building block to construct the supramolecular assemblies with distinctive properties. The possibility of non-covalent interactions ensures rich supramolecular chemistry of H<sub>2</sub>tba and H<sub>2</sub>ba compounds. On the other hand, the donor-acceptor features of these acids are important for the crystal design of pharmaceuticals, molecular recognition and catalytic activity [15]. It is of interest to obtain, study the structure and properties of salts which contain simultaneously two representatives of different pharmaceutically active classes, namely, fluoroquinolones and barbituric acids. The fundamental aim of the present work is to study the solid-state

pefloxacinium thiobarbiturate and pefloxacinium barbiturate structures. The molecular and supramolecular structures of fluoroquinolones with barbituric acids [16] which are currently absent in CSD are also useful. Here we report the synthesis data, IR spectra, and thermal stability of three salts, pefloxacinium 2-thiobarbiturate trihydrate,  $\text{PefH}_2(\text{Htba}) \cdot 3\text{H}_2\text{O}$  (**1**), pefloxacinium 2-thiobarbiturate,  $\text{PefH}_2(\text{Htba})$  (**2**) and bis(pefloxacinium 2-thiobarbiturate) hydrate,  $(\text{PefH}_2)_2(\text{Htba})_2 \cdot 2.56\text{H}_2\text{O}$  (**3**).

## 2. Experimental section

### 2.1. Reagents and synthesis

Pefloxacin (CAS 70458-92-3), thiobarbituric acid (CAS 504-17-6) and barbituric acid (CAS 67-52-7) with the purity  $\geq 98\%$  were obtained from Sigma-Aldrich and used as received. Compounds **1-3** were prepared by the crystallization from the aqueous solution. For the synthesis of **2**, the  $\text{PefH}$  (0.6 mmol) was dissolved in water ( $5 \text{ cm}^3$ ) at  $80^\circ\text{C}$ , then a solid  $\text{H}_2\text{tba}$  (0.6 mmol) was added to the resulting solution during stirring and the solution was kept at  $80^\circ\text{C}$  up to total dissolution of  $\text{H}_2\text{tba}$  ( $\text{pH}=4.2$ ). After it was slowly cooled firstly down to room temperature, and then down to  $4^\circ\text{C}$ . After 20 minutes, the pale porange precipitate formed as fine rectangular crystals was filtered off, washed with acetone and air dried to a constant mass. Yield was 53%. Single crystal of **1** (gold prism) was grown by the continuous filtrate evaporation at  $4^\circ\text{C}$  within 6 months. However, we could not get a sufficient amount of the single-phase compound **1**. Pale yellow compound **3** was prepared by a procedure analogous to that described for the preparation of **2**, but  $\text{H}_2\text{ba}$  ( $\text{pH}=4.6$ ) was used instead of  $\text{H}_2\text{tba}$ . Выход 43%. Crystal of **2** and **3**, suitable for single crystal X-ray diffraction analysis, were grown by filtrate corresponding evaporation at  $4^\circ\text{C}$ . Optical microscopy images of **2** and **3** crystals were obtained using a Nikon Eclipse LV100 Microscope and presented in Fig. 1S. Attempts to obtain other hydrates of these compounds by crystallization from an aqueous solution were unsuccessful.

Anal. Calc. for  $\text{C}_{21}\text{H}_{30}\text{FN}_5\text{O}_8\text{S}$ (**1**): C, 47.5; H, 5.69; N, 13.2; S, 6.03. Found: C, 48.0; H, 5.26; N, 13.6; S, 6.21%. Anal. Calc. for  $\text{C}_{21}\text{H}_{24}\text{FN}_5\text{O}_5\text{S}$ : C, 52.8; H, 5.07; N, 14.7; S, 6.72. Found: C, 52.5; H, 4.89; N, 14.3; S, 6.87% (**2**). Anal. Calc. for  $\text{C}_{42}\text{H}_{50}\text{F}_2\text{N}_{10}\text{O}_{14.56}$  (**3**): C, 52.2; H, 5.22; N, 14.5. Found: C, 51.8; H, 5.13; N, 14.7%.

### 2.2. X-ray diffraction analysis

The intensity patterns were collected from single crystals **1**, **2** and **3** using the SMART APEX II and D8 Venture X-ray single crystal diffractometers (Bruker AXS) equipped with a CCD-detector, graphite monochromator and  $\text{Mo K}\alpha$  radiation source. The absorption corrections

were applied using the SADABS program. The structures were solved by the direct methods using package SHELXS and refined in the anisotropic approach for non-hydrogen atoms using the SHELXL program [17]. All hydrogen atoms were found via Fourier difference maps. Further the hydrogen atoms which are linked with C,N atoms in the Htba<sup>-</sup>, Hba<sup>-</sup> and PefH<sup>+</sup> ions were positioned geometrically as riding on their parent atoms with  $d(\text{C-H}) = 0.93\text{-}0.98 \text{ \AA}$ ,  $d(\text{N-H}) = 0.86\text{-}0.89 \text{ \AA}$  depending on geometry and  $U_{\text{iso}}(\text{H}) = 1.2U_{\text{eq}}(\text{C,N})$ . All hydrogen atoms of the H<sub>2</sub>O molecules and one H atom in OH group of PefH<sup>+</sup> ion were refined with bond length restraint  $d(\text{O-H}) = 0.9 \text{ \AA}$  and  $U_{\text{iso}}(\text{H}) = 1.2U_{\text{eq}}(\text{O})$ . The structure test for the presence of missing symmetry elements and possible voids was produced using the program PLATON [18]. The DIAMOND program is used for the crystal structure plotting [19].

Powder X-ray diffraction data of **2** and **3** were obtained using diffractometer D8 ADVANCE (Bruker) equipped by a VANTEC detector with a Ni filter. The measurements were made using Cu K $\alpha$  radiation. The structural parameters defined by single crystal analysis were used as a basic in powder pattern Rietveld refinement. The refinement was produced using program TOPAS 4.2 [20]. Low *R*-factors and good refinement results shown in (Fig. 2S) indicate the crystal structures of the powder samples to be representative one of the **2** and **3** bulk structure.

### 2.3. Physical measurements

TGA was carried out on the simultaneous SDT-Q600 thermal analyzer (TA Instruments, USA) under dynamic air atmosphere (50 ml/min flow rate) within 22–350 °C at the scan rate of 10 °C/min. The qualitative composition of the evolved gases was determined by FT-IR spectrometer Nicolet380 (Thermo Scientific, USA) combined with a thermal analyzer and with the TGA/FT-IR interface (attachment for the gas phase analysis). This set up allows simultaneous accumulation of the DTA and TG data, and composition of the released gas phase. The compound weight was 5.603 mg for **2** and 6.302 mg for **3**. Platinum crucibles with perforated lids were used. The IR absorption spectra of the compounds in KBr were recorded over the range of 400–4000 cm<sup>-1</sup> at room temperature on a FT-IR spectrometer Nicolet 6700 (Thermo Scientific, USA, SFU CEJU).

## 3. Results and discussion

### 3.1. Crystal structures of (1)

The unit cell of the pefloxacinium 2-thiobarbiturate trihydrate, PefH<sub>2</sub><sup>+</sup>(Htba<sup>-</sup>)·3H<sub>2</sub>O (**1**), correspond to triclinic symmetry. Space group *P*-1 was determined from the statistical analysis of the reflection intensities. The main crystal data are shown in Table 1. The main bond lengths

and valence angles are shown in [Table 1S](#). They coincide with those given in the literature for the  $\text{PefH}_2^+$  ion [21-24] and  $\text{Htba}^-$  ion [25-29].

The independent part of the unit cell contains one  $\text{PefH}_2^+$  ion, one  $\text{Htba}^-$  ion and three  $\text{H}_2\text{O}$  molecules ([Fig. 1a](#)). There are two intramolecular hydrogen bonds C–H...F, O–H...O ([Figure 1a](#)) and nine intermolecular hydrogen bonds N–H...O, O–H...O in the structure ([Figure 2a, Table 2S](#)) which form 2D plane network. This is 5-nodal net with stoichiometry (3-c)(3-c)(3-c)(4-c)(5-c) and with vertex symbol (3.5.6.8<sup>2</sup>.9)(3.5.6<sup>2</sup>.7<sup>2</sup>.8<sup>3</sup>.9)(3.5.6)(5.6<sup>2</sup>)(5.8<sup>2</sup>) which is new [30].

Similar to **1**, the structures pefloxacinium methanesulfonate hydrates [22, 23] are also stabilized by hydrogen bonds involving the terminal piperazinyl N atom of the pefloxacinium and an O atom of the methanesulfonate ion, with strong N—H...O interactions and the carbonyl and carboxyl groups are also involved in a strong intramolecular O—H...O hydrogen bond. The H-bonds with the participation of two chains, each of which consists of two water molecules, bind two  $\text{Htba}^-$  ions together and lead to a synthon  $\text{R}_6^6(20)$ . Each  $\text{Htba}^-$  ion has two such ions in the nearest environment ([Figure 2a](#)).  $\text{PefH}_2^+$  is connected with two  $\text{H}_2\text{O}$  molecules and two  $\text{Htba}^-$  ions. In **1** the hydrogen bond donors are two N atom of thiobarbiturate ion, and the acceptors are two O atoms keto and carboxyl groups of  $\text{PefH}_2^+$  cation. The most interesting motifs in this network are  $\text{R}_3^3(10)$ ,  $\text{R}_6^4(12)$ ,  $\text{R}_6^5(14)$  and  $\text{R}_6^6(20)$  ([Figure 2a](#)). The  $\pi$ - $\pi$  interactions between  $\text{Htba}^-$  and  $\text{PefH}_2^+$  ions, and between two  $\text{PefH}_2^+$  ions (in a head-to-tail manner) are stabilized structure. Similar the packing of  $\text{PefH}_2^+$  ions observed in the structures of  $(\text{PefH}_2^+)\text{CH}_3\text{SO}_3^- \cdot 2\text{H}_2\text{O}$  [23]  $(\text{PefH}_2^+)\text{CH}_3\text{SO}_3^- \cdot 0.1\text{H}_2\text{O}$  [22] and  $(\text{PefH}_2^+)_2\text{PtCl}_4^{2-} \cdot 2\text{H}_2\text{O}$  [24], The  $\pi$ - $\pi$  interaction in **1** combines pefloxacinium cations to the pairs ([Table 3S, Fig. 3Sa](#)).

### 3.2. Crystal structures of (2)

The unit cell of  $\text{PefH}_2^+(\text{Htba}^-)$  (**2**) correspond to monoclinic symmetry. Space group  $P2_1/c$  was determined from the statistical analysis of the reflection intensities and extinction rules. The main crystal data are shown in [Table 1](#). The main bond lengths and valence angles are shown in [Table 1S](#). They coincide with those found earlier for **1** and given in the literature for ions  $\text{PefH}_2^+$  [21-24] and  $\text{Htba}^-$  [25-29].

The independent part of the unit cell contains one  $\text{PefH}_2^+$  ion, one  $\text{Htba}^-$  ion ([Figure 1b](#)). There are two intramolecular hydrogen bonds C–H...F, O–H...O ([Figure 1b](#)) and three intermolecular hydrogen bonds N–H...O in the structure ([Figure 2b, Table 2S](#)) which form chain along *a*-axis.  $\text{Htba}^-$  ion in **2** has direct H-bond to  $\text{PefH}_2^+$  like in  $\text{PefH}_2(\text{Htba}) \cdot 3\text{H}_2\text{O}$ . The number of intermolecular hydrogen bonds in compound **2** is much smaller in comparison with **1** due to absence of water molecules in compound, which can stabilize crystal structures when there is an imbalance in the number of acceptors and donors [31].  $\text{PefH}_2^+$  has two the hydrogen bond donors

(carboxylic acid, O–H; (CH<sub>3</sub>)NH<sup>+</sup> group) and six potentially strong hydrogen bond acceptors (three N- and three O-atoms). Htba<sup>−</sup> ion has potentially two hydrogen bond donors (two NH groups) and five acceptors (two O-, two N- and one S-atoms). In the **2** an imbalance in the number of donors and acceptors в PefH<sub>2</sub><sup>+</sup> are partly compensated by active participation in the hydrogen bonding of Htba<sup>−</sup> ion (Figure 2b). The structure **2** is stabilized by intermolecular hydrogen bonds N–H...O between Htba<sup>−</sup> ions forming a centrosymmetric homosynton R<sub>2</sub><sup>2</sup>(8) and C<sub>2</sub><sup>2</sup>(10), and besides Htba<sup>−</sup> ions form infinite chains along *a*-axis. Also, there are π–π interactions between two rings of PefH<sub>2</sub><sup>+</sup> in structure (Table 3S, Figure 3Sb). Contrary to **1**, the Htba<sup>−</sup> ions in compound **2** are not involved in π–π interaction. However, π–π interactions between two rings of PefH<sub>2</sub> joint them to the pairs in **2**.

### 3.3. Crystal structures of (3)

The unit cells of (PefH<sub>2</sub><sup>+</sup>)<sub>2</sub>(Hba<sup>−</sup>)<sub>2</sub>·2.56H<sub>2</sub>O (**3**) correspond to triclinic symmetry and space group *P*-1 was determined. The main crystal data are shown in Table 1. The main bond lengths and valence angles are shown in Table 1S.

The independent part of the unit cell contains two PefH<sub>2</sub><sup>+</sup> ions, two Hba<sup>−</sup> ions, one ordered water molecule and two disordered H<sub>2</sub>O molecules with partial occupations (Fig. 1c). Occupancies sum of all H<sub>2</sub>O in the independent part of unit cell equal to 2.562(4). Hydrogen bonding could not be analyzed in detail because H atoms of disordered water molecules were not found. Anyway, there are two intramolecular hydrogen bonds C–H...F, O–H...O (Figure 1c), six intermolecular hydrogen bonds N–H...O (Figure 2c) and at least one O–H...O bond in the structure (Table 2S) which form chain along *a*-axis. Hydrogen bond pattern is similar with pattern of **2** (Figure 2b). The dominantly formed hydrogen bonding in **3** is N–H...O interaction, which leads to a centrosymmetric synthon R<sub>2</sub><sup>2</sup>(8) and to formation of infinite chain from Hba<sup>−</sup> ions. Similar infinity chains from Htba<sup>−</sup> ions were observed in **2**. There are several π–π interactions between two rings of PefH<sub>2</sub><sup>+</sup> and Hba<sup>−</sup> (Table 3S, Fig. 3Sc).

### 3.4. IR spectroscopy

The IR spectra of PefH<sub>2</sub>(Htba) (**2**) and PefH<sub>2</sub>)<sub>2</sub>(Hba)<sub>2</sub>·2.56H<sub>2</sub>O (**3**) are displayed in Figure 6S. They are very difficult to interpret due to numerous bands in a particular frequency range less than 1500 cm<sup>−1</sup>. In the analysis of the IR spectra used the results of these studies [32–35]. The IR spectra of **2** (Figure 4S, curve 1) and **3** (Figure 4S, curve 2) markedly differ from spectra of initial reagents (PefH, H<sub>2</sub>tba or H<sub>2</sub>ba), which indicates the obtainment of new compounds. The very broad bands in the 3600–3400 cm<sup>−1</sup> can be assigned to stretching modes of NH and OH for PefH<sub>2</sub><sup>+</sup>, Htba<sup>−</sup> and Hba<sup>−</sup> ions. In the region of stretching vibrations C=O in IR spectra of Hba<sup>−</sup> ion the band with the highest frequency lies at 1688 cm<sup>−1</sup> [34]. In alkaline and alkali earth metals

(M) thiobarbiturate bond M–O is weak and predominantly ion-dipole in nature, therefore one can assume that stretching vibrations C=O which were found in IR spectra of these compounds can be attributed to uncoordinated Htba<sup>−</sup> ions. The most high frequency band  $\nu(\text{C}=\text{O})$  in sodium thiobarbiturate is located at  $1645\text{ cm}^{-1}$  [27], and in potassium thiobarbiturate it is located at  $1630\text{ cm}^{-1}$  [36]. Therefore, the band associated with  $\nu(\text{C}=\text{O})$  of Htba<sup>−</sup> and Hba<sup>−</sup> ions are located noticeably below  $1700\text{ cm}^{-1}$ . So the bands at  $1716\text{ cm}^{-1}$  for **2** and at  $1706\text{ cm}^{-1}$  for **3** correspond to the stretching vibration  $\nu(\text{C}=\text{O})$  in COOH [35], and this proves the protonation of the carboxyl group PefH and in agreement with X-ray single crystal data. Low frequency of another very strong absorption band  $\nu(\text{C}=\text{O})$  at  $1629\text{ cm}^{-1}$  in IR spectra of **2** and **3** can be explained by the participation of the O2 atom of PefH<sub>2</sub><sup>+</sup> in an intramolecular hydrogen bond O2–H...O1 (Figure 1b,c) and/or it is assigned  $\kappa \nu(\text{C}=\text{O})$  in Htba<sup>−</sup> and Hba<sup>−</sup> ions, respectively.

### 3.5. Thermal decomposition

According to TG curves, the mass of sample **2** remains unchanged up to  $\sim 270\text{ }^\circ\text{C}$  (Figure 5S), and there are no peaks in the DSC curve below this temperature. This confirms the anhydrous nature of the compound. The compound **2** melts with decomposition at  $T > 270\text{ }^\circ\text{C}$ . The decomposition is accompanied by an endo effect at  $275.3\text{ }^\circ\text{C}$ . The H<sub>2</sub>tba melts with decomposition at  $250.6\text{ }^\circ\text{C}$  [37], i.e. compound **2** is more thermal stable than H<sub>2</sub>tba. According to the IR spectroscopic analysis of evolved gases during thermolysis, the H<sub>2</sub>O, CO<sub>2</sub> and NH<sub>3</sub> are formed.

Both TG and DSC curves of **3** show two-step dehydration which is accompanied by two endo effects at  $124.7\text{ }^\circ\text{C}$  and  $244.1\text{ }^\circ\text{C}$  (Figure 6S). This is confirmed by the results of IR spectroscopic analysis of evolved gases, according to which, when heated to  $260\text{ }^\circ\text{C}$ , only dehydration of the substance takes place, what is more the dehydration with two steps. The first stage of dehydration in the range of  $60\text{--}150\text{ }^\circ\text{C}$  showed the weight loss ( $\Delta m$ ) equal to 4.1%, but the second stage in the range of  $235\text{--}260\text{ }^\circ\text{C}$  showed  $\Delta m = 1.8\%$ . Total weight loss (5.9%) is bigger than calculated weight loss taking in assumption total dehydration ( $-2.5\text{H}_2\text{O}$ ,  $\Delta m_{\text{theor}} = 4.66\%$ ). The observed difference can be explained by the partial overlap of the second stage of dehydration with the oxidative decomposition of the compound. The H<sub>2</sub>ba melts with decomposition at  $245.0\text{ }^\circ\text{C}$  [38], i.e. compound **3** is more thermal stable than H<sub>2</sub>ba. Oxidative decomposition products are H<sub>2</sub>O, CO<sub>2</sub>, SO<sub>2</sub>.

## 4. Conclusions

Crystallization of PefH with 2-thiobarbituric and barbituric acids resulted in the isolation of three new salts. Two intramolecular hydrogen bonds C–H...F, O–H...O (Figure 1) and intermolecular

hydrogen bonds N–H...O, O–H...O are stabilized the structures of **1-3** (Figure 2, Table 2S). The Htba<sup>−</sup> and Hba<sup>−</sup> ions are connected with PefH<sub>2</sub><sup>+</sup> only by intermolecular hydrogen bond N–H...O. In **1** the hydrogen bond donors are two N atom of thiobarbiturate ion, and the acceptors are two O atoms keto and carboxyl groups of PefH<sub>2</sub><sup>+</sup> cation. However in **2-3** the H-bond donor is the positively charged piperazinium N atom in PefH<sub>2</sub><sup>+</sup>, and the acceptor is one O atom keto group of Htba<sup>−</sup> or Hba<sup>−</sup> ions. The dominantly formed hydrogen bonding in **2-3** is N–H...O interaction, which leads to a centrosymmetric synthon R<sub>2</sub><sup>2</sup>(8) and the forming of infinite chains of Htba<sup>−</sup> or Hba<sup>−</sup> ions. Fluoroquinolones have potentially two strong hydrogen bond donors and 6-7 potentially strong hydrogen bond acceptors [39]. An imbalance in the number of donors and acceptors in fluoroquinolone salts can be compensated by incorporating water molecules into crystal lattices (as in **1**). Water molecules stabilize crystal structures by forming a diverse arrangement of supramolecular heterosynthons [40]. Another way of compensation of an imbalance in donors/acceptors ratio is the inclusion in the composition of fluoroquinolone salts of anions capable of self-association, for example, the Htba<sup>−</sup> and Hba<sup>−</sup> ions, as in **2** and **3**. The structures **1-3** are stabilized by  $\pi$ – $\pi$  interactions between PefH<sub>2</sub><sup>+</sup> ions of the head-to-tail type. These interactions connect PefH<sub>2</sub><sup>+</sup> ions in pairs in **1-2** or in infinite chains in **3** (Table 3S, Fig.2S). Also there are  $\pi$ – $\pi$  interactions between Htba<sup>−</sup> and PefH<sub>2</sub><sup>+</sup> ions in **1**. IR spectra data are in agreement with X-ray single crystal diffraction analysis. Compounds **2** and **3** were found to be more thermal stable than H<sub>2</sub>tba and H<sub>2</sub>ba acids, respectively.

### Supplementary data

The crystallographic data (excluding structure factors) for the structural analysis have been deposited with Cambridge Crystallographic Data Centre ((**1**) - CCDC 1537391; (**2**) - CCDC 1537392; (**3**) - CCDC 1537393). The information may be obtained free of charge from The Director, CCDC, 12 Union Road, Cambridge CB2 1EZ, UK (Fax: +44(1223)336-033, E-mail: deposit@ccdc.cam.ac.uk, or www: www.ccdc.cam.ac.uk).

### Acknowledgements

The study was carried out within the public task of the Ministry of Education and Science of the Russian Federation to the Siberian Federal University (4.7666.2017/BP) in 2017-2019. V.V.A. is grateful to the Ministry of Education and Science of the Russian Federation for the financial support of the investigation. X-ray data from single crystals were obtained with use the analytical equipment of Baikal Center of collective use of SB RAS and with use the analytical equipment of Krasnoyarsk Center of collective use of SB RAS.



## References

1. Padeiskaya E.N. Prevention, Diagnosis, and Pharmacotherapy of Some Infectious Diseases (Bioinform, Moscow, 2002) (in Russian)
2. Mitsner L.A. Chem. Rev. 105 (2005) 559.
3. Zhang C.-L., Wang Y. J. Chem. Eng. Data. 53 (2008) 1295-1297.
4. Goodman L.S., Gilman A. (1970) Pharmacological Basis of Therapeutics, The MacMillan Company, London: 98–132
5. A. I. Rakhimov, S. A. Avdeev, Le Thi Doan Chang // Russ. J. General Chem., 2009, Vol. 79, No. 2, pp. 338–339.
6. Levina R.Ya., Velichko F.K. (1960) Advances in the chemistry of barbituric acids. Russ. Chem. Rev. 29(8): 437–459
7. Bojarski J.T., Mokrosz J.L., Barton H.J., Paluchowska M.H. (1985) Recent progress in barbituric acid chemistry. Adv. Heterocycl. Chem. 38: 229–297
8. Ahluwalia V.K., Aggarwal R. (1996) Chemistry of thiobarbituric acid. Proc. Ind. Nat. Sci. Acad. A 62(5): 369–413
9. Braga D., Cadoni M., Grepioni F., Maini L., Rubini K. CrystEngComm. 8 (2006) 756–760.
10. Mendez E., Cerda M.F., Gancheff J.S., Torres J., Kremer C., Castiglioni J., Kieninger M., Ventura O.N. J. Phys. Chem. C. 2007. V. 111. N 8. P. 3369–3383.
11. T.C. Lewis, D.A. Tocher, S.L. Price, Cryst. Growth Des. 4 (2004) (5) 979-987
12. Zencirci N., Gstrein E., Langes C., Griesser U.J. Thermochim. Acta 485 (2009) 33-42.
13. Schmidt M.U., Brüning J., Glinnemann J., Hützler M.W., Mörschel P., Ivashevskaya S.N., Streek J., Braga D., Maini L., Chierotti M.R., Gobetto R. Angew. Chem. Int. Ed. 50 (2011) 7924-7926
14. Chierotti M.R., Ferrero L., Garino N., Gobetto R., Pellegrino L., Braga D., Grepioni F., Maini L. Chem. Eur. J. 2010. V.16. P.4347 – 4358.
15. K.T. Mahmudov, M.N. Kopylovich, A.M. Maharramov, M.M. Kurbanova, A.V. Gurbanov, A.J.L. Pombeiro, Coord. Chem. Rev. 265 (2014) 1.
16. Cambridge Structural Database, Version 5.37, Univ. of Cambridge, Cambridge, UK, 2015
17. G.M. Sheldrick, *Acta Cryst. A*, 2008, **64**, 112–122.
18. PLATON – A Multipurpose Crystallographic Tool. Utrecht University, Utrecht, The Netherlands, 2008.
19. K. Brandenburg, M. Berndt, DIAMOND - Visual Crystal Structure Information System CRYSTAL IMPACT, Postfach 1251, D-53002 Bonn
20. Bruker AXS TOPAS V4: General profile and structure analysis software for powder diffraction data. – User’s Manual, Bruker AXS, Karlsruhe, Germany, 2008.
21. Fun H.-K., Hemamalini M., Shetty D.N., Narayana B., Eathirajan H.S. *Acta Cryst.* E66 (2010) o714
22. Parvez M., Arayne M.S., Sultana N., Siddiqi A.Z. *Acta Cryst.* C56 (2000) 910.
23. Toffoli, P., Rodier, N., Ceolin, R. & Blain, Y. *Acta Cryst.* C43 (1987) 1745–1748.
24. Toffoli, P., Khodadad P., Rodier, N.. *Acta Cryst.* C44 (1988) 470
- [25] N.N. Golovnev, M.S. Molokeev, *Acta Crystallogr.* C69 (7) (2013) 704.
- [26] N.N. Golovnev, M.S. Molokeev, S.N. Vereshchagin, V.V. Atuchin, *J. Coord. Chem.* 66 (23) (2013) 4119.
- [27] N.N. Golovnev, M.S. Molokeev, S.N. Vereshchagin S.N., V.V. Atuchin, M.Y. Sidorenko, M.S. Dmitrushkov, *Polyhedron* 70 (1) (2014) 71.
- [28] N.N. Golovnev, M.S. Molokeev, *Russ. J. Inorg. Chem.* 59 (9) (2014) 943.
- [29] N.N. Golovnev, M.S. Molokeev, *Russ. J. Coord. Chem.* 40 (9) (2014) 564.
- [30] V.A. Blatov; A.P. Shevchenko; D.M. Proserpio. *Crystal Growth & Design.*, **14**, 3576 (2014).
- [31] Clarke H.D., Arora K.K., Bass H., Kavuru P., Ong T.T., Pujari T., Wojtas L., Zaworotko M.J. *Cryst. Growth. Des.* 10 (2010) 2152-2167.
- [32] N.A. Smorygo, B.A. Ivin, *Khim. Geterotsikl. Soedin.* 10 (1975) 1402.

- [33] J.T. Bojarski, J.L. Mokrosz, H.J. Barton, M.H. Paluchowska, *Adv. Heterocycl. Chem.* 38 (1985) 229.
- [34] H.C. Garcia, F.B. de Almeida, R. Diniz, M.I. Yoshida, L.F.C. de Oliveira, *J. Coord. Chem.* 64 (2011) 1125.
- [35] [Dorofeev V.L. *Pharmaceutical Chemistry Journal.* 38 (2004) (12) 693-697.
- [36] N.N. Golovnev, M.S. Molokeevev, and M.Y. Belash, *J. Struct. Chem.*, 2013, **54**(3), 566–570.
- [37] N.N. Golovnev, M.S. Molokeevev, L.S. Tarasova, V.V. Atuchin, N.I. Vladimirova, *J. Mol. Struct.* 2014. V.1068. P. 216–221
- [38]. Chierotti M.R., Gaglioti K., Gobetto R., Braga D., Grepioni F., Maini L. *CrystEngComm.* – 2013. – **15**. – P. 7598–7605.
- [39] I. Turel, *Coord. Chem. Rev.* 232 (2002) 27–47.
- [40] Desiraju R.J., *J. Chem. Soc.. Chem. Commun.* (1991) 426-428.

## **Graphical Abstract**

**Table 1.** Crystal structure parameters of **1-3**

Single crystal	PefH <sub>2</sub> (Htba)·3H <sub>2</sub> O ( <b>1</b> )	PefH <sub>2</sub> (Htba) ( <b>2</b> )	(PefH <sub>2</sub> ) <sub>2</sub> (Hba) <sub>2</sub> ·2.56H <sub>2</sub> O ( <b>3</b> )
Moiety formula	C <sub>21</sub> H <sub>30</sub> FN <sub>5</sub> O <sub>8</sub> S	C <sub>21</sub> H <sub>24</sub> FN <sub>5</sub> O <sub>5</sub> S	C <sub>42</sub> H <sub>50</sub> F <sub>2</sub> N <sub>10</sub> O <sub>14.56</sub>
Dimension (mm)	0.2×0.16×0.05	0.20×0.30×0.35	0.43×0.20×0.17
Color	Pale orange	Pale yellow	Pale yellow
Molecular weight	531.56	477.51	965.88
Temperature (K)	150	150	296
Space group, <i>Z</i>	<i>P</i> -1, 2	<i>P</i> 2 <sub>1</sub> / <i>c</i>	<i>P</i> -1, 2
<i>a</i> (Å)	8.4651 (6)	12.0768 (9)	10.3252 (3)
<i>b</i> (Å)	9.3753 (6)	14.7120 (11)	13.8631 (4)
<i>c</i> (Å)	15.8077 (9)	12.2222 (9)	16.9586 (3)
$\alpha$ (°)	89.484 (2)	90	101.243 (1)
$\beta$ (°)	88.735 (2)	95.109 (3)	92.514 (1)
$\gamma$ (°)	78.147 (2)	90	109.471 (1)
<i>V</i> (Å <sup>3</sup> )	1227.48 (14)	2162.9 (3)	2229.1 (1)
$\rho_{\text{calc}}$ (g/cm <sup>3</sup> )	1.438	1.466	1.439
$\mu$ (mm <sup>-1</sup> )	0.196	0.204	0.115
Reflections measured	11838	105889	24769
Reflections independent	5647	6337	10127
Reflections with <i>F</i> > 4 $\sigma$ ( <i>F</i> )	3139	4737	7257
2 $\theta_{\text{max}}$ (°)	55.27	60.16	55.02
<i>h, k, l</i> - limits	-10 ≤ <i>h</i> ≤ 10; -12 ≤ <i>k</i> ≤ 12; -20 ≤ <i>l</i> ≤ 18	-17 ≤ <i>h</i> ≤ 17; -20 ≤ <i>k</i> ≤ 20; -17 ≤ <i>l</i> ≤ 17	-13 ≤ <i>h</i> ≤ 13; -17 ≤ <i>k</i> ≤ 17; -15 ≤ <i>l</i> ≤ 22
<i>R</i> <sub>int</sub>	0.0473	0.0869	0.0278
The weighed refinement of <i>F</i> <sup>2</sup>	$w=1/[\sigma^2(F_o^2)+(0.0628P)^2]$	$w=1/[\sigma^2(F_o^2)+(0.0570P)^2+1.4849P]$	$w=1/[\sigma^2(F_o^2)+(0.1137P)^2+0.3971P]$
Number of refinement parameters	346	303	637
<i>R</i> 1 [ <i>F</i> <sub>o</sub> > 4 $\sigma$ ( <i>F</i> <sub>o</sub> )]	0.0523	0.0468	0.0550
<i>wR</i> 2	0.1060	0.1116	0.1704
<i>Goof</i>	0.905	1.060	1.039
$\Delta\rho_{\text{max}}$ (e/Å <sup>3</sup> )	0.416	0.893	0.626
$\Delta\rho_{\text{min}}$ (e/Å <sup>3</sup> )	-0.287	-0.328	-0.373
( $\Delta/\sigma$ ) <sub>max</sub>	0.001	0.001	0.001

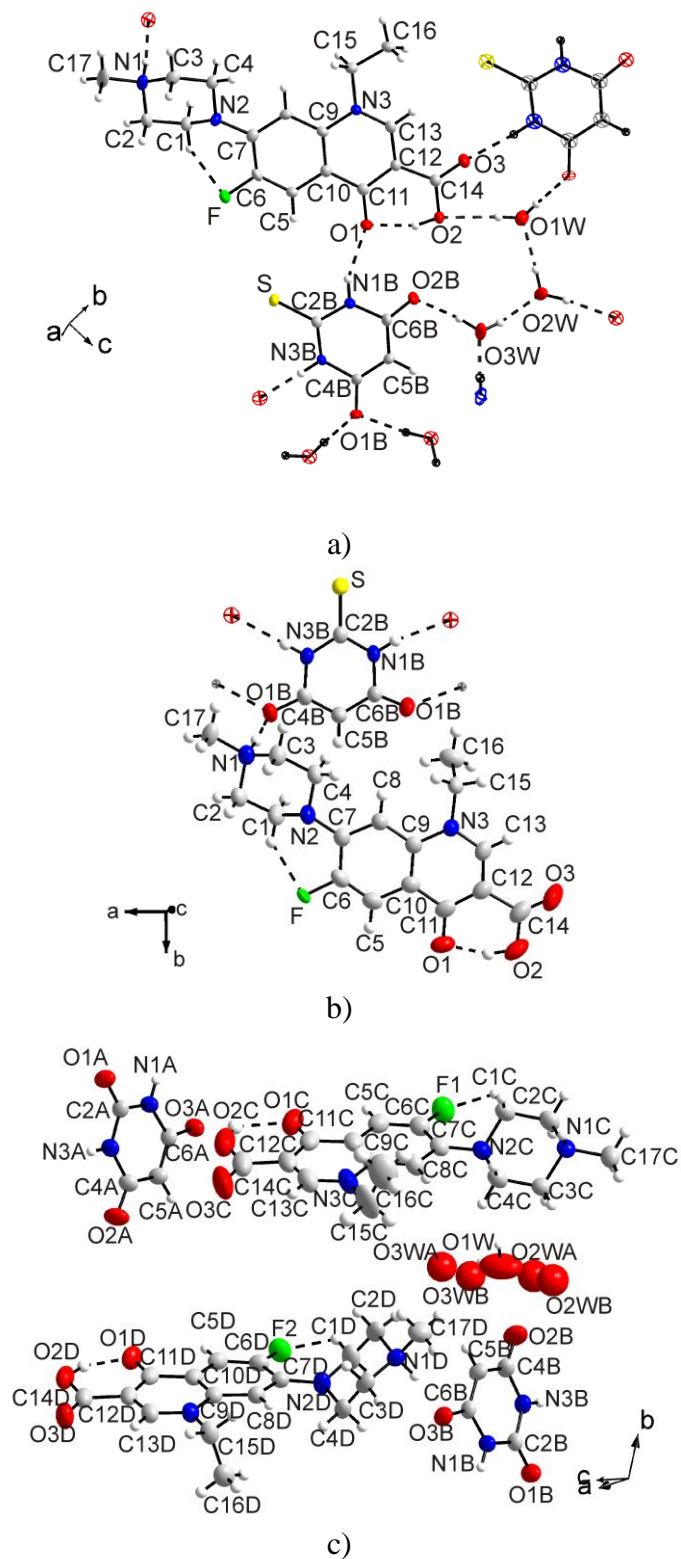
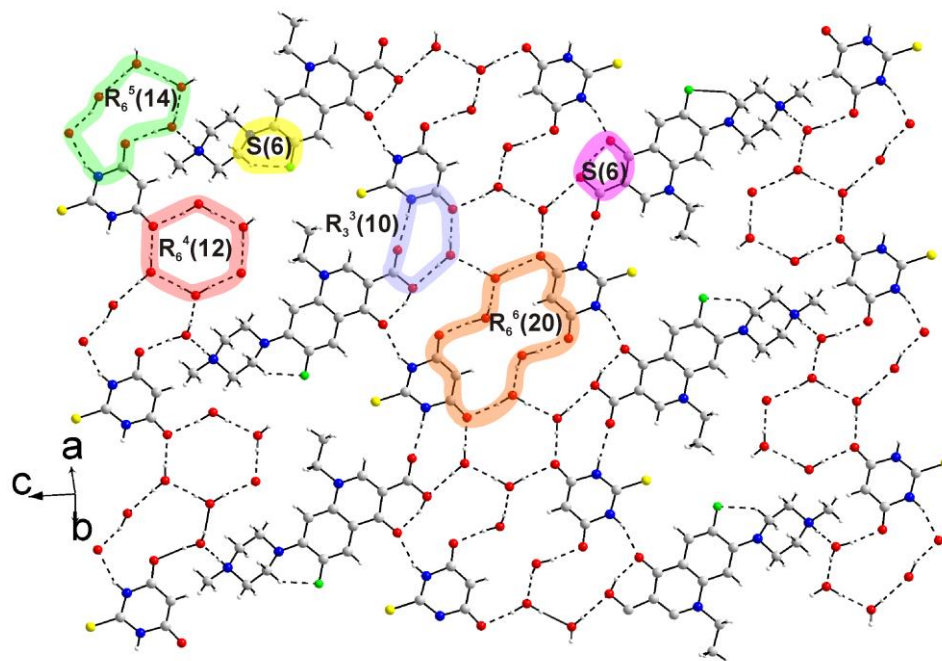
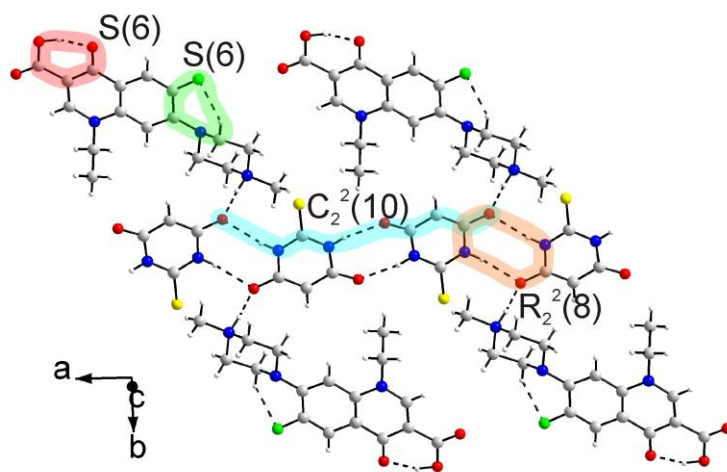


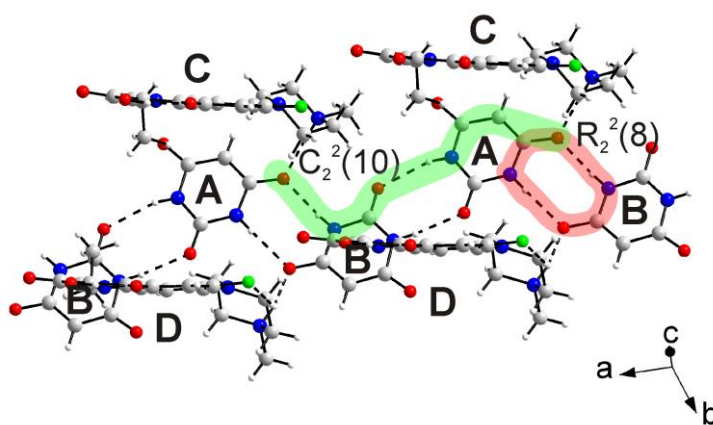
**Figure 1.** The asymmetric unit of the  $\text{PefH}_2(\text{Htba})\cdot 3\text{H}_2\text{O}$  (**1**) (a),  $\text{PefH}_2(\text{Htba})$  (**2**) and  $(\text{PefH}_2)_2(\text{Hba})_2\cdot 2.56\text{H}_2\text{O}$  (**3**) (c) unit cell. All atoms in the asymmetric unit are labeled. The neighboring symmetry-generated atoms are represented by principal ellipsoids with an individual color. The bonds linking asymmetric unit atoms with the symmetry-generated atoms and intermolecular hydrogen bonds are represented by dashed lines. The ellipsoids are drawn at the 50% probability level, except for the hydrogen atoms represented by spheres.



a)



b)



c)

**Figure 2.** Hydrogen bonding in **1** (a), **2** (b) and **3** (c). The H-bonds are marked by dashed lines, the H-bond motifs are marked by circles. Different Hba<sup>-</sup> ions are marked by A, B labels and PefH<sub>2</sub><sup>+</sup> ions are marked by C, D labels in (**3**) (c).

## Supported Information

**Table 1S.** Main geometric parameters (Å, °) of **(1-3)**

Geometry of pefloxacinium ion							
PefH <sub>2</sub> (Htba)·3H <sub>2</sub> O <b>(1)</b>		PefH <sub>2</sub> (Htba) <b>(2)</b>		(PefH <sub>2</sub> ) <sub>2</sub> (Hba) <sub>2</sub> ·2.56H <sub>2</sub> O <b>(3)</b>			
F—C6	1.354 (3)	F—C6	1.360 (2)	F1—C6C	1.355 (2)	F2—C6D	1.354 (2)
O1—C11	1.269 (3)	O1—C11	1.265 (2)	O1C—C11C	1.263 (3)	O1D—C11D	1.271 (2)
O2—C14	1.331 (3)	O2—C14	1.337 (2)	O2C—C14C	1.327 (4)	O2D—C14D	1.329 (3)
O3—C14	1.215 (3)	O3—C14	1.208 (2)	O3C—C14C	1.191 (4)	O3D—C14D	1.195 (3)
N1—C17	1.488 (3)	N1—C17	1.487 (2)	N1C—C17C	1.489 (2)	N1D—C17D	1.493 (3)
N1—C2	1.490 (3)	N1—C2	1.495 (2)	N1C—C2C	1.484 (3)	N1D—C2D	1.496 (3)
N1—C3	1.493 (3)	N1—C3	1.494 (2)	N1C—C3C	1.487 (2)	N1D—C3D	1.491 (2)
N2—C7	1.394 (3)	N2—C7	1.399 (2)	N2C—C7C	1.405 (2)	N2D—C7D	1.373 (2)
N2—C1	1.471 (3)	N2—C1	1.476 (2)	N2C—C1C	1.473 (2)	N2D—C4D	1.461 (3)
N2—C4	1.457 (3)	N2—C4	1.464 (2)	N2C—C4C	1.458 (2)	N2D—C1D	1.462 (2)
N3—C13	1.336 (3)	N3—C13	1.335 (2)	N3C—C13C	1.329 (3)	N3D—C13D	1.339 (2)
N3—C9	1.403 (3)	N3—C9	1.394 (2)	N3C—C9C	1.400 (3)	N3D—C9D	1.392 (2)
N3—C15	1.495 (3)	N3—C15	1.480 (2)	N3C—C15C	1.497 (4)	N3D—C15D	1.484 (2)
C1—C2	1.513 (3)	C1—C2	1.514 (2)	C1C—C2C	1.507 (3)	C1D—C2D	1.501 (3)
C3—C4	1.515 (4)	C3—C4	1.509 (2)	C3C—C4C	1.501 (3)	C3D—C4D	1.509 (3)
C5—C6	1.358 (3)	C5—C6	1.355 (2)	C5C—C6C	1.360 (3)	C5D—C6D	1.354 (3)
C5—C10	1.410 (3)	C5—C10	1.410 (2)	C5C—C10C	1.400 (3)	C5D—C10D	1.402 (3)
C6—C7	1.413 (4)	C6—C7	1.423 (2)	C6C—C7C	1.408 (3)	C6D—C7D	1.418 (3)
C7—C8	1.389 (4)	C7—C8	1.390 (2)	C7C—C8C	1.382 (3)	C7D—C8D	1.391 (2)
C8—C9	1.401 (3)	C8—C9	1.397 (2)	C8C—C9C	1.402 (3)	C8D—C9D	1.403 (2)
C9—C10	1.407 (3)	C9—C10	1.402 (2)	C9C—C10C	1.400 (3)	C9D—C10D	1.407 (3)
C10—C11	1.438 (3)	C10—C11	1.447 (2)	C10C—C11C	1.454 (3)	C10D—C11D	1.442 (3)
C11—C12	1.422 (3)	C11—C12	1.427 (2)	C11C—C12C	1.424 (4)	C11D—C12D	1.422 (3)
C12—C13	1.382 (3)	C12—C13	1.372 (2)	C12C—C13C	1.368 (4)	C12D—C13D	1.363 (3)
C12—C14	1.475 (3)	C12—C14	1.483 (2)	C12C—C14C	1.496 (3)	C12D—C14D	1.486 (3)
C15—C16	1.504 (4)	C15—C16	1.513 (2)	C15C—C16C	1.474 (5)	C15D—C16D	1.511 (3)

Geometry of thiobarbiturate and barbiturate ions							
PefH <sub>2</sub> (Htba)·3H <sub>2</sub> O <b>(1)</b>		PefH <sub>2</sub> (Htba) <b>(2)</b>		(PefH <sub>2</sub> ) <sub>2</sub> (Hba) <sub>2</sub> ·2.56H <sub>2</sub> O <b>(3)</b>			
S—C2B	1.659 (3)	S—C2B	1.686 (2)	O1A—C2A	1.231 (2)	O1B—C2B	1.233 (2)
O1B—C4B	1.268 (3)	O1B—C4B	1.274 (2)	O2A—C4A	1.247 (2)	O2B—C4B	1.249 (2)
O2B—C6B	1.249 (3)	O2B—C6B	1.241 (2)	O3A—C6A	1.276 (2)	O3B—C6B	1.275 (2)
N1B—C2B	1.353 (3)	N1B—C2B	1.349 (2)	N1A—C2A	1.364 (2)	N1B—C2B	1.366 (2)
N1B—C6B	1.405 (3)	N1B—C6B	1.409 (2)	N1A—C6A	1.387 (2)	N1B—C6B	1.385 (2)
N3B—C2B	1.364 (3)	N3B—C2B	1.346 (2)	N3A—C2A	1.358 (2)	N3B—C2B	1.355 (2)

N3B—C4B	1.393 (3)	N3B—C4B	1.401 (2)	N3A—C4A	1.394 (2)	N3B—C4B	1.387 (2)
C4B—C5B	1.386 (3)	C4B—C5B	1.383 (2)	C4A—C5A	1.403 (2)	C4B—C5B	1.398 (3)
C5B—C6B	1.401 (4)	C5B—C6B	1.409 (2)	C5A—C6A	1.378 (2)	C5B—C6B	1.386 (3)
C2B— N1B—C6B	126.2 (2)	C2B— N1B—C6B	124.7 (1)	C2A— N1A—C6A	124.0 (1)	C2B— N1B—C6B	124.2 (1)
N1B— C2B—N3B	114.4 (2)	N1B— C2B—N3B	116.2 (1)	N1A— C2A—N3A	115.9 (2)	N1B— C2B—N3B	115.7 (2)
N3B— C2B—S	123.0 (2)	N3B— C2B—S	121.2 (1)	N3A— C2A—O1A	122.6 (2)	N31B— C2B—O1B	122.7 (2)
C2B— N3B—C4B	125.5 (2)	C2B— N3B—C4B	125.0 (1)	C2A— N3A—C4A	125.1 (1)	C2B— N3B—C4B	125.3 (1)
N1B— C2B—S	122.7 (2)	N1B— C2B—S	122.6 (1)	N1A— C2A—O1A	121.6 (2)	N1B— C2B—O1B	121.6 (2)
C4B— C5B—C6B	121.6 (2)	C4B— C5B—C6B	121.4 (1)	C4A— C5A—C6A	121.6 (2)	C4B— C5B—C6B	121.5 (2)

**Table 2S.** Hydrogen-bond geometry in (1-3) structures (Å, °)

D—H	d(D—H)	d(H...A)	∠ D—H...A	D...A	A	Transformation for A atom
PefH <sub>2</sub> (Htba)·3H <sub>2</sub> O (1)						
N1—H0	0.98	1.66	166	2.621 (3)	O3W	x, y, -1+z
N1B—H1B	0.86	1.99	156	2.795 (3)	O1	x, y, z
N3B—H3B	0.86	1.98	175	2.836 (3)	O3	1+x, -1+y, z
O2—H2	0.88 (3)	1.69 (3)	158 (3)	2.534 (3)	O1	x, y, z
C1—H01A	0.97	2.21	124	2.867 (3)	F	x, y, z
O1W—H11W	0.86 (3)	1.90 (3)	176 (2)	2.759 (4)	O1B	1+x, 1+y, z
O1W—H12W	0.86 (3)	2.22 (3)	173 (3)	3.066 (3)	O2	x, y, z
O2W—H21W	0.90 (3)	2.84 (3)	171 (3)	2.734 (3)	O1B	2-x, 1-y, 1-z
O2W—H22W	0.87 (3)	1.88 (3)	176 (2)	2.747 (3)	O1W	x, y, z
O3W—H31W	0.84 (3)	1.86 (3)	169 (3)	2.693 (3)	O2W	x, y, z
O3W—H32W	0.87 (2)	1.76 (3)	172 (3)	2.622 (3)	O2B	x, y, z
PefH <sub>2</sub> (Htba) (2)						
N1—H0	0.98	1.73	175	2.705 (2)	O1B	x, y, z
N1B—H1B	0.86	1.99	169	2.835 (2)	O2B	1-x, 1-y, 1-z
N3B—H3B	0.86	2.09	155	2.892 (2)	O1B	2-x, -y, -z
O2—H2	0.96 (2)	1.57 (2)	159 (2)	2.492 (2)	O1	x, y, z
C1—H01A	0.97	2.21	127	2.893 (2)	F	x, y, z
(PefH <sub>2</sub> ) <sub>2</sub> (Hba) <sub>2</sub> ·2.56H <sub>2</sub> O (3)						

---

N1C—H0C	0.98	1.69	174	2.672 (2)	O3A	x, y, z
N1D—H0D	0.98	1.71	166	2.672 (2)	O3B	x, y, z
N1A—H1A	0.86	2.12	178	2.979 (2)	O3B	x, 1+y, z
N1B—H1B	0.86	1.98	174	2.838 (2)	O3A	x, -1+y, z
N3A—H3A	0.86	2.15	163	2.984 (2)	O1B	1+x, 1+y, z
N3B—H3B	0.86	2.00	169	2.845 (2)	O1A	-1+x, -1+y, z
O2C—H2C	0.91 (4)	1.94 (3)	123 (3)	2.550 (3)	O1C	x, y, z
O2D—H2D	0.91 (2)	1.69 (2)	151 (3)	2.523 (3)	O1D	x, y, z
C1C—H1BC	0.97	2.27	124	2.927 (2)	F1	x, y, z
O1W—H12W	0.92	1.91 (3)	158 (3)	2.787 (3)	O2A	x, y, z

---



**Table 3S.** Parameters of the  $\pi$ - $\pi$  interaction in (1-3)

$Cg_i-Cg_j$	$d(Cg-Cg), \text{Å}$	$\alpha, \text{deg}$	$\beta, \text{deg}$	$\gamma, \text{deg}$	$Cg_{i-p}, \text{Å}$	Shift, $\text{Å}$
PefH <sub>2</sub> (Htba)·3H <sub>2</sub> O (1)						
$Cg_1 - Cg'_1$	3.491 (2)	0.0 (1)	13.4	13.4	3.396 (1)	0.808
$Cg_1 - Cg'_2$	3.824 (2)	0.3 (1)	27.3	27.0	3.407 (1)	1.736
$Cg_2 - Cg'_3$	3.969 (2)	5.9 (1)	26.0	25.4	3.587 (1)	1.699
PefH <sub>2</sub> (Htba) (2)						
$Cg_{1A} - Cg'_{1B}$	3.654 (2)	4.9 (2)	14.4	17.5	3.484 (2)	1.102
$Cg_{1A} - Cg'_{2B}$	3.843 (3)	5.4 (2)	25.1	24.7	3.490 (2)	1.609
$Cg_{2A} - Cg'_{1B}$	3.914 (3)	1.8 (2)	25.6	25.4	3.536 (2)	1.678
$Cg_{2A} - Cg_3$	4.007 (2)	6.7 (2)	22.3	27.8	3.771 (2)	1.355
$Cg_{2B} - Cg_4$	3.894 (2)	3.6 (2)	24.9	25.7	3.509 (2)	1.688
(PefH <sub>2</sub> ) <sub>2</sub> (Hba) <sub>2</sub> ·2.56H <sub>2</sub> O (3)						
$Cg_{1C} - Cg'_{1C}$	3.988 (1)	0.0 (1)	29.9	29.9	3.4576 (9)	1.988
$Cg_{1C} - Cg'_{2D}$	3.520 (1)	5.6 (1)	13.0	18.5	3.3383 (9)	1.116
$Cg_{1D} - Cg'_{2C}$	3.593 (1)	3.4 (1)	16.4	13.8	3.4891 (8)	0.858
$Cg_{1D} - Cg'_{1D}$	3.597 (1)	0.00 (9)	22.6	22.6	3.3208 (8)	1.382
$Cg_{1D} - Cg''_{2D}$	3.687 (1)	3.25 (9)	23.4	25.2	3.3349 (7)	1.572

(1):  $Cg_1$  and  $Cg_2$  are the centers of the rings in PefH<sup>+</sup>.  $Cg_3$  is the center of the ring Htba<sup>-</sup>.  $Cg'_1$  was obtained from  $Cg_1$  by the transform (1-x,1-y,-z),  $Cg'_2$  was obtained from  $Cg_2$  by the transform (1-x,1-y,-z),  $Cg'_3$  was obtained from  $Cg_3$  by the transform (2-x,1-y,-z).  $Cg_{i-p}$  is the distance between the center of the ring  $Cg_i$  in the  $\pi$ - $\pi$  interaction.

(2):  $Cg_{1C}$ ,  $Cg_{2C}$  and  $Cg_{1D}$ ,  $Cg_{2D}$  are the centers of the rings in PefH<sup>+</sup>.  $Cg'_{1C}$  was obtained from  $Cg_{1C}$  by the transform (1-x,1-y,-z),  $Cg'_2$  was obtained from  $Cg_2$  by the transform (1-x,1-y,-z).

(3):  $Cg_1$  and  $Cg_2$  are the centers of the rings in PefH<sup>+</sup>.  $Cg'_1$  was obtained from  $Cg_1$  by the transform (1-x,2-y,1-z),  $Cg'_{2D}$  was obtained from  $Cg_{2D}$  by the transform (1-x,1-y,1-z),  $Cg'_{2C}$  was obtained from  $Cg_{2C}$  by the transform (1-x,1-y,1-z),  $Cg'_{1D}$  was obtained from  $Cg_{1D}$  by the transform (2-x,1-y,1-z),  $Cg''_{1D}$  was obtained from  $Cg_{1D}$  by the transform (2-x,1-y,1-z).

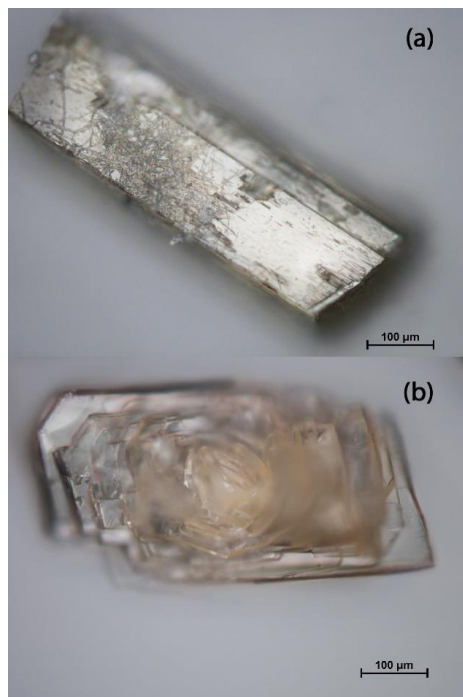


**Figure 1S.** Optical microscope images of (a) –  $(\text{PefH}_2)_2(\text{Hba})_2 \cdot \text{H}_2\text{O}$ ; (b) -  $\text{PefH}_2(\text{Htba})$  crystals

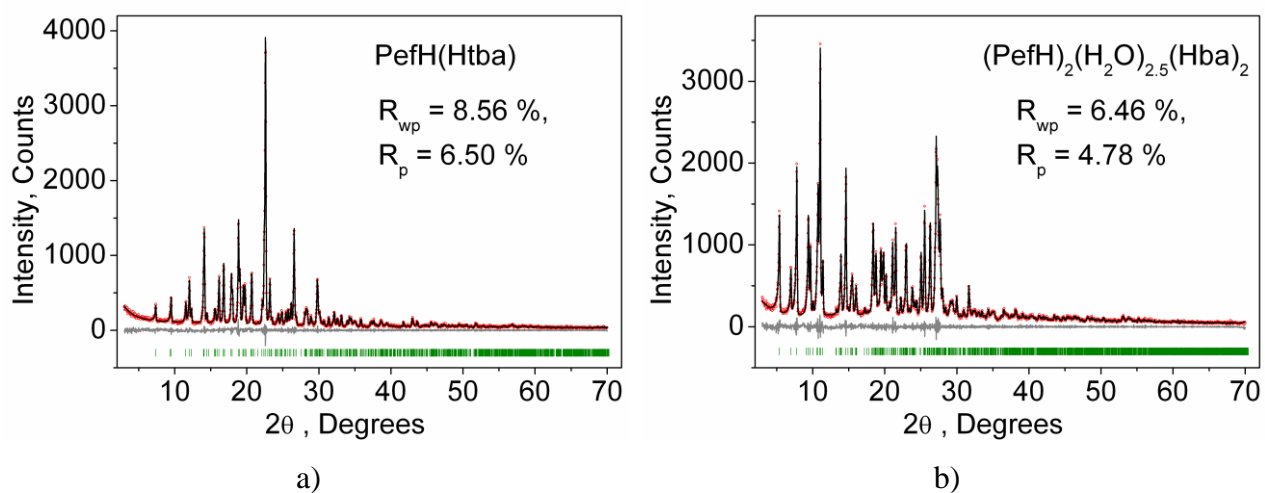


**Figure 2S.** Difference X-ray powder patterns of  $\text{PefH}_2(\text{Htba})$  (a) and  $(\text{PefH}_2)_2(\text{Hba})_2 \cdot 2.56\text{H}_2\text{O}$  (b).

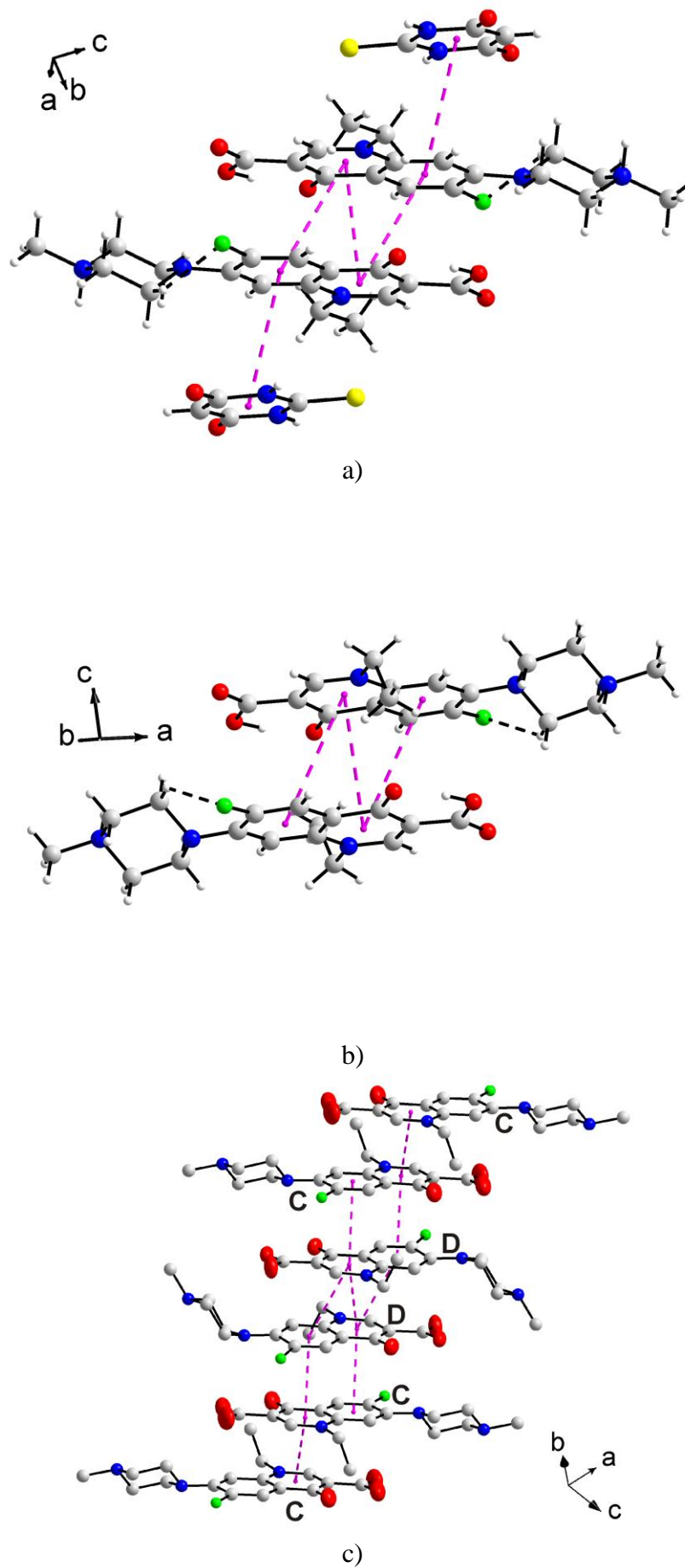


**Figure 3S.**  $\pi$ - $\pi$  interactions the  $\text{Htba}^- \dots \text{PefH}_2^+$ , and  $\text{PefH}_2^+ \dots \text{PefH}_2^+$  ions in **1** (a), between the  $\text{PefH}_2^+$  ions in **(2)** (b) and between the  $\text{PefH}^+$  ions in **(3)** (c).

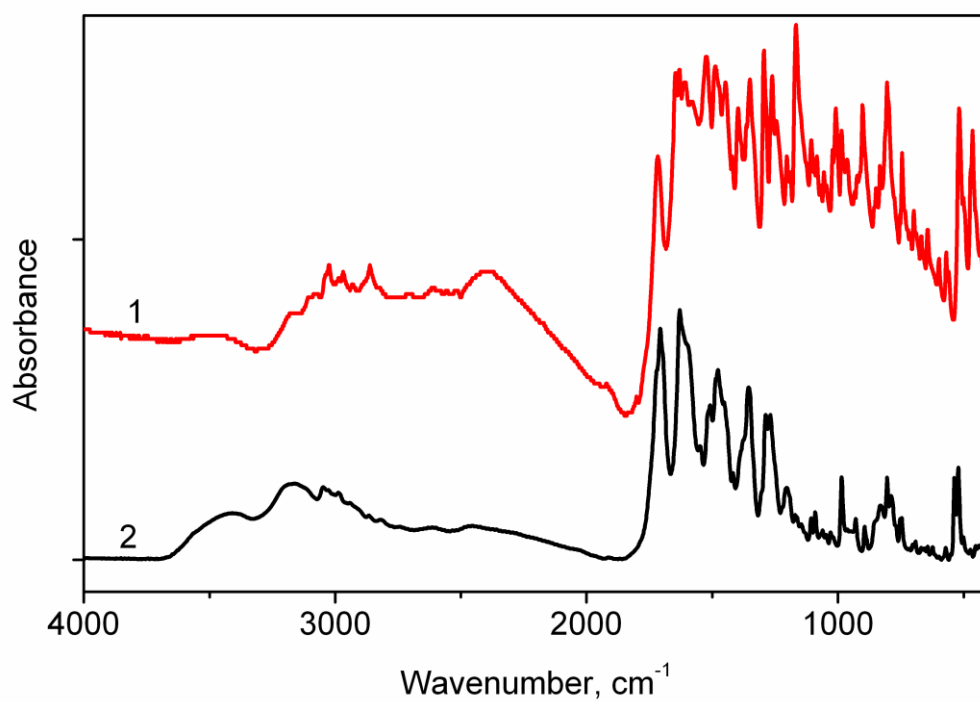


**Figure 4S.** IR-spectra of PefH<sub>2</sub>(Htba) (1), (PefH<sub>2</sub>)<sub>2</sub>(Hba)<sub>2</sub>·2.56H<sub>2</sub>O (2)

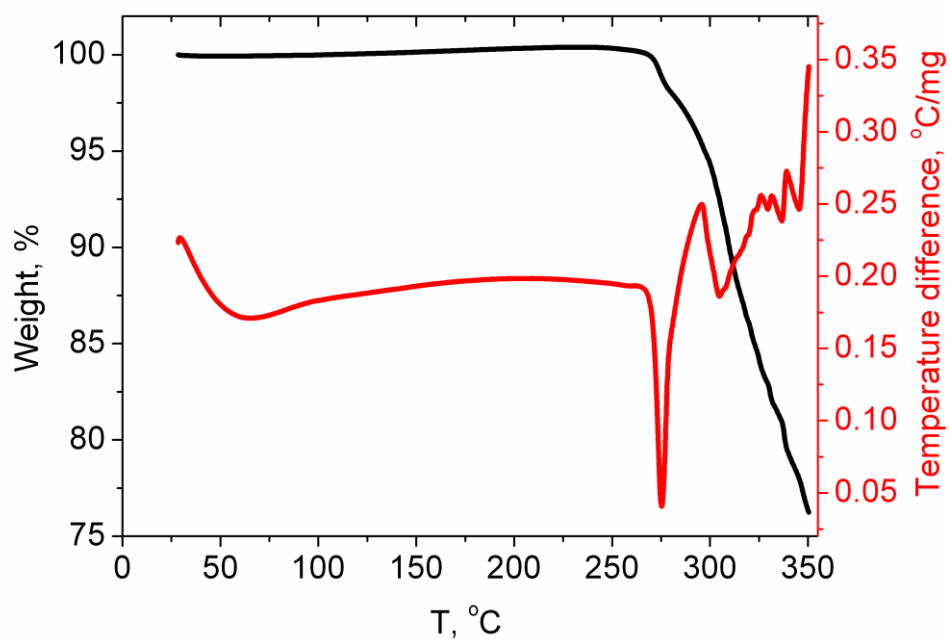


**Figure 5S.** TG and DSC curves of 2. Dynamic air atmosphere

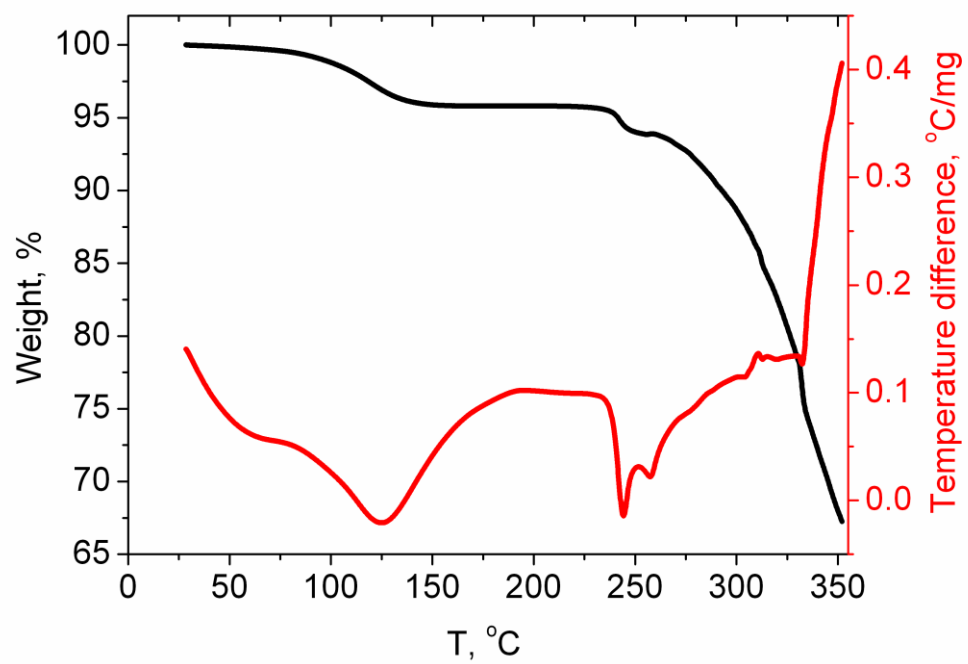


**Figure 6S.** TG and DSC curves for thermal decomposition of **3** under air atmosphere